Amphoteric Lewis acid/base activity enables an unprecedented pathway for low-energy C-O cleavage in the electrocatalytic reduction of carbon dioxide

Hemlata Agarwala[‡,1], Xiaoyu Chen[‡,2], Julien R. Lyonnet[†1], Ben A. Johnson[1], Mårten Ahlquist[*,2], Sascha Ott[*,1]

[1]Department of Chemistry – Ångström Laboratory, Uppsala University, Box 523, 751 20 Uppsala, Sweden; [2]Department of Theoretical Chemistry and Biology, School of Engineering Sciences in Chemistry, Biotechnology and Health, KTH Royal Institute of Technology, 10691 Stockholm, Sweden.

KEYWORDS. molecular electrocatalysis, catalytic mechanism, ruthenium polypyridyl, metallacyclic intermediate, spectroscopy, DFT calculations.

ABSTRACT: Molecular electrocatalysts for CO_2-to-CO conversion often operate at large overpotentials, with the cleavage of a C-O bond in the [metal-CO_2]$^{n+}$ intermediate largely contributing to this unfavorable phenomenon. In natural CO dehydrogenase enzymes as well as synthetic systems, it has been shown that additional Lewis acids can aid in weakening the C-O bond by *O*-coordination. Illustrated with ruthenium-based CO_2 reduction electrocatalysts, [(*t*Bu$_3$tpy)(pp)**Ru**(CH$_3$CN)]$^{2+}$ (*t*Bu$_3$tpy = 4,4′,4′′-tri-*tert*-butyl-2,2′:6′,2′′-terpyridine; pp = bidentate polypyridine), we herein present computational and experimental evidence for a mechanistic route that involves *one* metal center that acts as both Lewis base *and* Lewis acid at different stages of the catalytic cycle. The Lewis basic character of the **Ru** center manifests itself in the initial nucleophilic attack at the CO_2 substrate to form [**Ru**-CO_2]^0, while its Lewis acid character allows for the formation of a 5-membered metallacyclic intermediate, [**Ru**-CO_2CO_2]^{0,c}, by intramolecular cyclization of a linear [**Ru**-CO_2CO_2]^0 species that is formed from [**Ru**-CO_2]^0 and a second equivalent of CO_2. The pathway is enabled by the flexible ligation of polypyridine ligands that liberate coordination sites upon demand. The cyclic intermediate, [**Ru**-CO_2CO_2]^{0,c}, is crucial for energy-conserving turnover, as it allows for a third reduction at a more positive potential than that of the starting complex **Ru**$^{2+}$. The calculated activation barrier for C-O bond cleavage in [**Ru**-CO_2CO_2]$^{-1,c}$ is dramatically decreased to merely 10.5 kcal mol^{-1} as compared to the 60 kcal mol^{-1} required for C-O bond cleavage in the non-cyclic [**Ru**-CO_2CO_2]^0 adduct. The ruthenacyclic intermediates have been characterized experimentally by FTIR and ^{13}C NMR spectroscopy during electrocatalytic turnover and been corroborated by density functional theory (DFT) investigations. The present report is the first of its kind that experimentally observes metallacyclic intermediates during catalytic turnover in electrocatalytic CO_2 reduction, offering a new design feature that can be implemented consciously in future catalyst designs.

INTRODUCTION

Electrochemical reduction of CO_2 can assist in mitigating atmospheric CO_2 levels and offer scalable means to store renewable electricity in energy dense compounds such as CO. Unfortunately, the electrochemical conversion of CO_2 to CO typically suffers from high overpotentials[1-3] that impede efficient implementation. In molecular transition metal-based catalysts, three key steps have been identified as potential kinetic bottlenecks: 1) CO_2 binding to the catalyst that is accompanied by bending of linear CO_2, 2) cleavage of a C-O bond in the [metal-CO_2]$^{n+}$ adduct and 3) CO dissociation from the catalyst. Of these three steps, the current report focuses mainly on C-O bond cleavage by molecular catalysts. Excessive electrochemical reduction steps have been shown to facilitate this process, but they typically occur at more negative standard potentials, thus leading to high overpotentials.[4-6] In nature, carbon monoxide dehydrogenase enzymes (CODH) can efficiently and reversibly convert CO to CO_2.[7] In the active site of CODH from the anaerobic bacterium *C. hydrogenoformans*, there is a [Ni-4Fe-5S] cluster, called the *C*-cluster, which consists of a [Ni-3Fe-4S] cubane linked to a unique Fe site through a sulfide.[8,9] In this cluster, Ni is the redox active center to which CO_2 binds. In close proximity is a redox inactive Fe(III) Lewis acid that facilitates C-O cleavage by stabilizing the OH^- group formed during the process.[9] Artificial systems attempt to mimic this function and the simple addition of Brønsted acids is frequently reported to enhance catalytic activity.[4,5,10-20] Also, several metal complexes with intramolecular Brønsted acidic groups positioned close to the reactive center have been shown to facilitate C-O cleavage.[3,21-33]

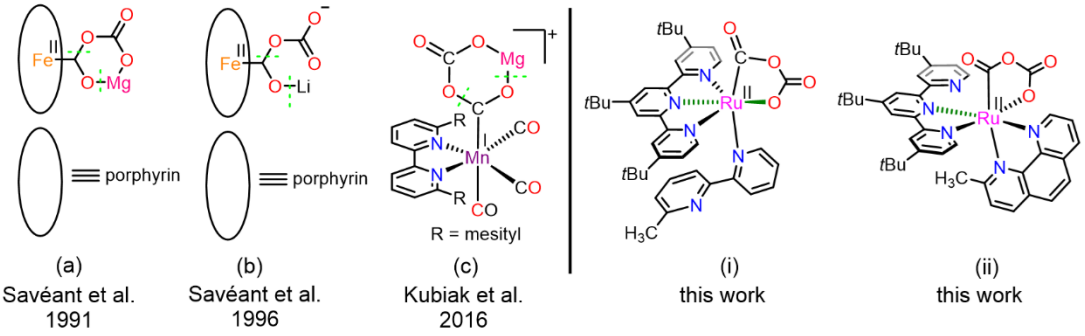

Figure 1. Representations of some transition metal-bound CO_2 adducts: (a-c) previously proposed,[34-37] stabilized by Lewis acid (LA) cations like Mg^{2+} and Li^+; (i and ii) investigated in the present work. The dashed green lines (----) indicate the scission of C-O and O-LA bonds in the subsequent step of the respective catalytic cycles.

Examples of catalytic rate enhancements for CO_2 electroreduction by Lewis acidic metal ions in molecular catalysts are comparatively rare.[34,35,37] In some of these systems, cyclic intermediates that comprise the catalytic metal center, two molecules of CO_2 and an exogenous alkali or alkaline earth metal Lewis acid have been proposed (Figure 1); however, to the best of our knowledge, none was observed experimentally.[34-37] It has been postulated that C-O cleavage from these cyclic intermediates is more facile compared to the systems without the additional Lewis acid.

Herein, we report an unprecedented pathway for C-O bond cleavage in the overall reductive disproportionation of CO_2 to CO and CO_3^{2-} that requires neither excessive catalyst reductions nor external Lewis acids. We present computational and experimental evidence for a mechanistic route that involves *one* metal center that acts as both Lewis base and Lewis acid at different stages of the catalytic cycle. The pathway is enabled by the flexible ligation of polypyridine ligands that can liberate coordination sites upon demand.

RESULTS AND DISCUSSION

The aforementioned mechanism is exemplified on two Ru-based catalysts, $[Ru(t\mathrm{Bu_3tpy})(CH_3bpy)(CH_3CN)]^{2+}$ ($\mathbf{1}^{2+}$)[38,39] and $[Ru(t\mathrm{Bu_3tpy})(CH_3phen)(CH_3CN)]^{2+}$ ($\mathbf{2}^{2+}$) (Scheme 1; $t\mathrm{Bu_3tpy}$ = 4,4′,4″-tri-*tert*-butyl-2,2′:6′,2″-terpyridine; CH_3bpy = 6-methyl-2,2′-bipyridine, CH_3phen = 2-methyl-1,10-phenanthroline) that differ in the bidentate ligand motif.

Scheme 1. Pictorial representation of complexes $\mathbf{1}^{2+}$ and $\mathbf{2}^{2+}$ (*cis* and *trans* isomers), and their two-electron reduced CO_2 adducts $[\mathbf{1}\text{-}CO_2]^0$ and $[\mathbf{2}\text{-}CO_2]^0$, respectively.

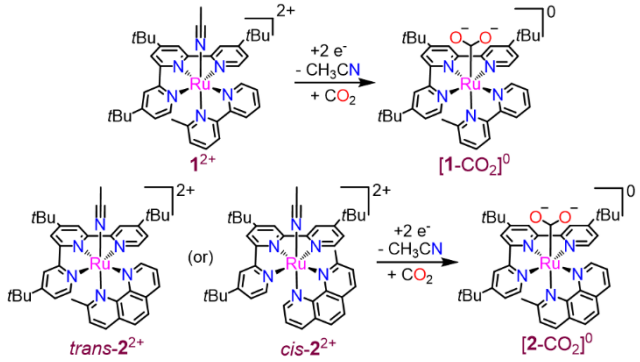

The bidentate phenanthroline in $\mathbf{2}^{2+}$ is a stronger coordinating ligand than 2,2′-bipyridine in $\mathbf{1}^{2+}$. The presence of the methyl group *ortho* to the nitrogen in the bidentate ligand is motivated by our previous finding that it labilizes the coordinated CH_3CN upon one-electron reduction of the complex.[38,39]

Complexes $\mathbf{1}^{2+}$ and $\mathbf{2}^{2+}$ were prepared from $Ru^{III}(t\mathrm{Bu_3tpy})(Cl)_3$ and the respective bidentate ligand by slight modifications of published procedures[40] (see ESI for details). While $\mathbf{1}^{2+}$ is isolated solely in its *trans* form[38] (Scheme 1, top), the NMR spectrum of $\mathbf{2}^{2+}$ (Figure S4) indicates the presence of two coordination isomers that differ in the position of the methyl group in the bidentate ligand with respect to the coordinated CH_3CN (depicted as *cis*-$\mathbf{2}^{2+}$ and *trans*-$\mathbf{2}^{2+}$ in Scheme 1).

As mentioned above, owing to the *ortho* methyl groups of the bidentate ligand, both complexes can liberate the CH_3CN ligand upon one-electron reduction.[38] The coordinatively unsaturated intermediate acts as a Lewis base towards CO_2, ultimately leading to the two-electron reduced CO_2 adducts $[\mathbf{1}\text{-}CO_2]^0$ and $[\mathbf{2}\text{-}CO_2]^0$ (Scheme 1) which are the starting points of the present study. In case of $[\mathbf{2}\text{-}CO_2]^0$, DFT calculations indicate that both isomers of $\mathbf{2}^{2+}$ lead to the *trans*-$[\mathbf{2}\text{-}CO_2]^0$ isomer shown in Scheme 1, as the nucleophilic attack of the reduced, pentacoordinate Ru center on CO_2 occurs from the sterically least occupied side of the complex (Scheme S1).

The cyclic voltammograms (CVs) of complexes $\mathbf{1}^{2+}$ and $\mathbf{2}^{2+}$ show electrochemically reversible one-electron reductions under argon at −1.76 V and −1.77 V *vs*. $Fc^{+/0}$ respectively (Figure 2, Table S1). Upon addition of CO_2 (0.28 M)[41], the first reductions become irreversible with noticeable enhancement in cathodic current, indicative of the electrochemical disproportionation of CO_2 to CO and carbonate.

As discussed above, C-O bond cleavage is one of the kinetic bottlenecks in CO_2 reduction chemistry, and mechanistic details of this step have hitherto been elusive for $[\mathbf{1}\text{-}CO_2]^0$ and $[\mathbf{2}\text{-}CO_2]^0$. It is well documented for related systems that in the absence of any exogenous Lewis acids such as protons or metal salts, the oxygen of the metal-bound CO_2 is sufficiently nucleophilic to attack a second CO_2 molecule.[42]

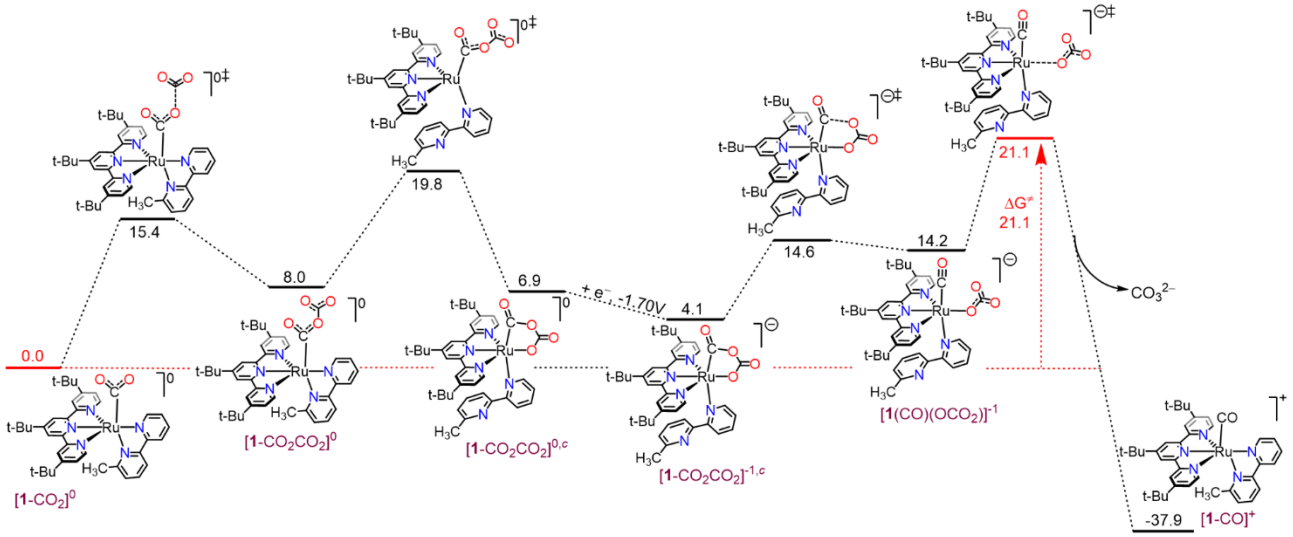

Figure 3. DFT-calculated pathway from $[\mathbf{1}\text{-}CO_2]^0$ to CO_3^{2-} *via* the cyclic three-electron reduced intermediate $[\mathbf{1}\text{-}COOCO_2]^{-1,c}$ at an applied potential of −1.82 V *vs.* $Fc^{+/0}$ in CH_3CN.

DFT calculations show that this is also the preferred pathway for $[\mathbf{1}\text{-}CO_2]^0$ and $[\mathbf{2}\text{-}CO_2]^0$, thereby producing $[\mathbf{1}\text{-}CO_2CO_2]^0$ and $[\mathbf{2}\text{-}CO_2CO_2]^0$, respectively (Figures 3 and 4). The activation energy ($\Delta G^{\ddagger}$) for this step is calculated to be 15.4 kcal mol^{-1} and 10.9 kcal mol^{-1} for $[\mathbf{1}\text{-}CO_2]^0$ and $[\mathbf{2}\text{-}CO_2]^0$, respectively, with corresponding reaction free energies of 8.0 kcal mol^{-1} and 4.1 kcal mol^{-1}.

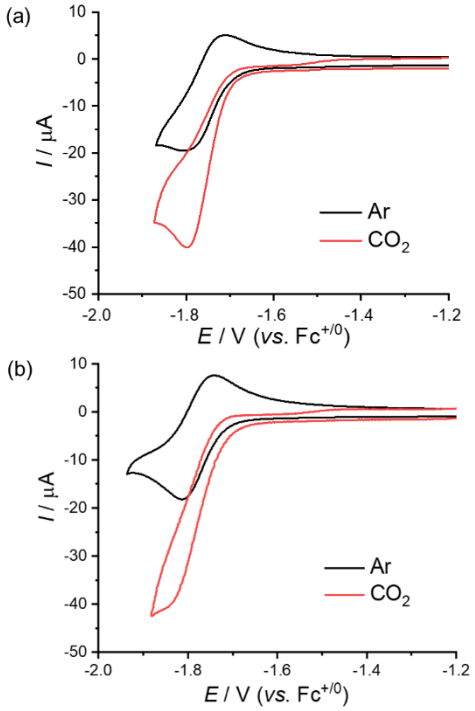

Figure 2. Cyclic voltammograms (shown is the first reduction) under Ar (black) and CO_2 (red; 0.28 M) of 1.0 mM solutions of (a) $\mathbf{1}(PF_6)_2$ and (b) $\mathbf{2}(PF_6)_2$. ν = 0.1 V s^{-1}, CH_3CN/0.1 M $TBAPF_6$.

While $[\mathbf{1}\text{-}CO_2CO_2]^0$ is a plausible intermediate in the catalytic cycle, direct C-O bond cleavage to produce CO_3^{2-} and the carbonyl complex (Scheme S2(a)) is not a viable option, as the calculated $\Delta G^{\ddagger}$ for this reaction is extremely high (60.5 kcal mol^{-1}). Moreover, electrochemical reduction of $[\mathbf{1}\text{-}CO_2CO_2]^0$ to further weaken the aforementioned C-O bond is also unlikely because the calculated standard potential at −2.13 V (*vs.* $Fc^{+/0}$) is significantly more negative than the applied potential (−1.82 V *vs.* $Fc^{+/0}$)[38]. Alternatively, the negatively charged terminal oxygen in $[\mathbf{1}\text{-}CO_2CO_2]^0$ could potentially attack the Ru center of a second 5-coordinate intermediate that is obtained by dissociation of CH_3CN from one-electron reduced $\mathbf{1}^+$.[38] Such an attack would form a bimetallic intermediate with a -C(O)O-C(O)O- bridge (Scheme S2(b)), similar to the one proposed for $Re^I(bpy)(CO)_3X$ catalysts.[43-45] However, this scenario is unlikely as well given that the catalytic current shows a first order dependence on catalyst concentration in the range 0.05 mM to 1.0 mM as reported previously.[38]

In the absence of any other established literature pathway, we hypothesized whether a structural reorganization of the complex, either to facilitate C-O bond cleavage or to drive a third reduction at a more positive potential, could provide an energetically plausible pathway. A closer inspection of $[\mathbf{1}\text{-}CO_2CO_2]^0$ shows that both the $-CO_2CO_2$ and the CH_3bpy are bidentate ligands. Hence, the possibility of a ligand exchange between the equatorial pyridine of CH_3bpy and the terminal oxygen of $-CO_2CO_2$ to form $[\mathbf{1}\text{-}CO_2CO_2]^{0,c}$ (Figure 3) was explored. The reaction was found to have a $\Delta G^{\ddagger}$ of 11.8 kcal mol^{-1}, with $[\mathbf{1}\text{-}CO_2CO_2]^{0,c}$ being more stable than $[\mathbf{1}\text{-}CO_2CO_2]^0$ by 1.1 kcal mol^{-1} (Figure 3). The C-O bond that needs to be cleaved is elongated from 1.36 Å (in $[\mathbf{1}\text{-}CO_2CO_2]^0$) to 1.42 Å (in $[\mathbf{1}\text{-}CO_2CO_2]^{0,c}$), indicating enhanced single bond character.

Cyclic 5-membered metallacycles of this kind are not entirely unprecedented and have been reported in the reaction of low-valent metal species with CO_2, albeit in a *stoichiometric* fashion.[46-52] In context of catalytic CO_2 conversion, a related Co-based metallacycle was recently proposed by Lloret-Fillol and co-workers, however without any experimental evidence.[6] Partial de-coordination of polydentate polypyridyl ligands from metal centers upon reduction have also been postulated earlier by some groups.[53-55]

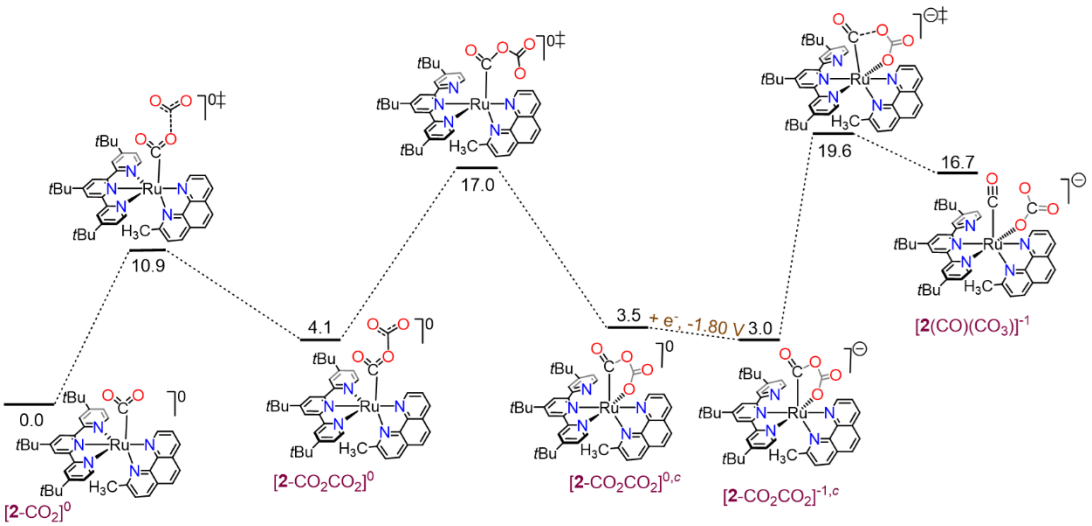

Figure 4. DFT calculated pathway to [2(CO)(CO₃)]⁻ *via* the cyclic three-electron reduced intermediate [2-CO₂CO₂]$^{-1,c}$ at an applied potential of -1.82 V *vs.* Fc$^{+/0}$ in CH₃CN.

However, the synergistic occurrence of these two processes in a single catalytic framework is, to the best of our knowledge, unprecedented.

The formation of the cyclic intermediate [**1**-CO₂CO₂]^{0,c} has another interesting aspect − the intramolecular Lewis acid stabilization of the negative charge at the terminal O by the Ru center may facilitate another reduction step from [**1**-CO₂CO₂]^{0,c} to [**1**-CO₂CO₂]$^{-1,c}$. Indeed, the potential for this reduction was calculated to be −1.70 V (*vs.* Fc$^{+/0}$ in CH₃CN), thus more positive than the calculated standard potential of the [**1**-CO₂CO₂]$^{-}$/[**1**-CO₂CO₂]^{0} couple by 430 mV, and more importantly, also more positive than the experimental applied potential of −1.82 V (Figure 3). [**1**-CO₂CO₂]$^{-1,c}$ is the lowest-energy intermediate in the later stages of the mechanism, and is proposed as the species from which C-O bond cleavage occurs.

The structure of [**1**-CO₂CO₂]$^{-1,c}$ is similar to that of [**1**-CO₂CO₂]^{0,c}, with a relatively long C-O bond that is to be cleaved. The formation of the metallacycle also induces some strain, that further weakens the C-O bond, as evidenced by the small O-Ru-C angle of 79.7° in [**1**-CO₂CO₂]$^{-1,c}$. The transition state for C-O cleavage was located just 10.5 kcal mol^{-1} above [**1**-CO₂CO₂]$^{-1,c}$, resulting in [**1**(CO)(OCO₂)]$^{-1}$ at 14.2 kcal mol^{-1} relative to [**1**-CO₂]^{0}. Dissociation of carbonate then proceeds with an activation energy at 21.1 kcal mol^{-1} relative to [**1**-CO₂]^{0}, accompanied by restoration of the bidentate coordination mode of CH₃bpy to Ru (Figure 3).

The highest activation energy barriers in Figure 3 are for the formation of [**1**-CO₂CO₂]^{0,c} at 19.8 kcal mol^{-1} and the release of carbonate at a similar free energy of 21.1 kcal mol^{-1}. The barriers agree well with the experimental TOF of 1.8 s^{-1} which corresponds to an activation free energy of 17.2 kcal mol^{-1} (see ESI for details).[38]

Having identified the flexible coordination of the bidentate ligand and the subsequent formation of the [**1**-CO₂CO₂]$^{-1,c}$ metallacycle as crucial features for efficient C-O bond cleavage, focus was directed towards the phenanthroline analogue [**2**-CO₂]^{0}. As expected from the strong coordinating ability of the 2-Mephen ligand to the metal center, calculations show that partial de-coordination of the phenanthroline ligand is not feasible. However, the system has the possibility to find another pathway for the formation of a related cyclic [**2**-CO₂CO₂]^{0,c}. This can be achieved by liberation of one of the pyridine units of the *t*Bu₃tpy ligand of [**2**-CO₂CO₂]^{0} instead (Figure 4). In analogy to the situation in [**1**-CO₂CO₂]^{0,c}, the intramolecular Lewis acid-base reaction that leads to the cyclic intermediate [**2**-CO₂CO₂]^{0,c} also allows access to a further reduction at a potential (Figure 4) that is less negative than that of the first reduction. The result is the three-electron reduced, cyclic adduct [**2**-CO₂CO₂]$^{-1,c}$ which is found as the lowest energy intermediate in the catalytic cycle (Figure 4) just before C-O bond cleavage.

The relatively high computed stabilities of the cyclic intermediate [**1**-CO₂CO₂]$^{-1,c}$ and even more so [**2**-CO₂CO₂]$^{-1,c}$ indicated that their spectroscopic observation during electrocatalytic CO₂ reduction might be feasible for the first time. Experimentally, the relevant region in the infra-red (IR) spectra is convoluted by the evolution of three major bands at 1684 cm^{-1}, 1645 cm^{-1} and 1304 cm^{-1} that arise from the CO_3^{2-}/HCO_3^{-} reductive disproportionation products (Figure 5a).[38,56] Nevertheless, the evolution of a weak shoulder at 1740 cm^{-1} along with some unresolvable structured transitions near 1230 cm^{-1} can be observed in the IR spectrum during the controlled potential electrolysis (CPE) of a 1.0 mM solution of **1**$^{2+}$ in anhydrous CH₃CN under CO₂ (0.28 M) (Figure 5a)[38]. DFT calculations show that these two absorptions most likely arise from a symmetric and an asymmetric C=O stretching vibration that are however ambiguous to assign to one particular species.[57] Both [**1**-CO₂]^{0} (calc. at 1730 cm^{-1} and 1235 cm^{-1}; Figure S3(a)) and [**1**-CO₂CO₂]$^{-1,c}$ (calc. at 1759 cm^{-1} and 1265 cm^{-1}; Figure S3(b)) exhibit calculated IR vibrations that match the experimentally observed ones.

IR spectra recorded during the CPE of **2**$^{2+}$ at −1.82 V (*vs.* Fc$^{+/0}$) under CO₂ (0.28 M) display the evolution of clearly visible bands at 1735, 1612 and 1272 cm^{-1} along with those of the CO_3^{2-}/HCO_3^{2-} byproduct (Figure 5b). The 1735 cm^{-1} band can be explained by a C=O stretching vibration in either [**2**-CO₂]^{0}

or [**2**-CO_2CO_2]^{0,c}; (calc: 1729 cm^{-1} and 1760 cm^{-1}, respectively; Figures S4a and S4c), while no absorption is expected for [**2**-CO_2CO_2]$^{-1,c}$ in this range. The experimental IR absorption at 1272 cm^{-1} corresponds very well to computed C-O stretches at 1253 cm^{-1} and 1291 cm^{-1} for [**2**-CO_2CO_2]^{0,c} and [**2**-CO_2CO_2]$^{-1,c}$, respectively (Figures S4c and S4d[58]), while the experimentally obtained peak at 1612 cm^{-1} is only found in the calculated IR spectrum of [**2**-CO_2CO_2]$^{-1,c}$ at 1614 cm^{-1} (Figures 5b and S4d).

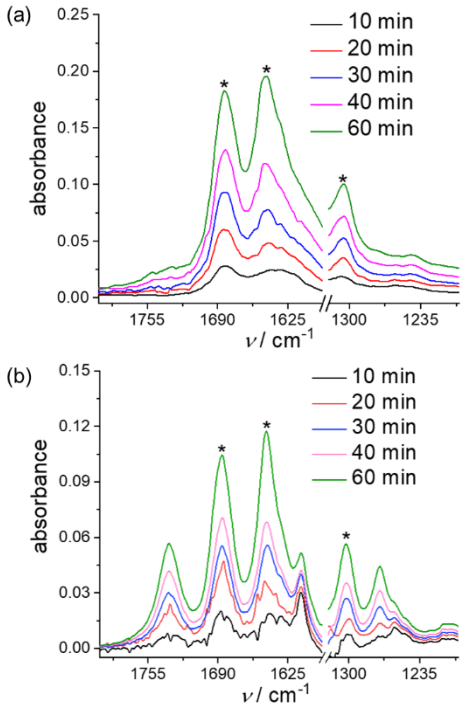

Figure 5. Fourier transformed infra-red (FT-IR) absorbance spectra of aliquots taken during controlled potential electrolysis of CO_2 saturated (0.28 M) solutions of (a) 1$(PF_6)_2$ (1.0 mM) and (b) 2$(PF_6)_2$ (1.0 mM), in anhydrous CH_3CN/0.1 M $TBAPF_6$ at an applied potential of −1.82 V (*vs.* $Fc^{+/0}$). The peaks marked with * arise from the CO_3^{2-}/HCO_3^{2-}.

This unique absorption allows for the identification of [**2**-CO_2CO_2]$^{-1,c}$ as one of the intermediates accumulated during CPE. Altogether, the IR monitoring indicates the presence of [**2**-CO_2]^0, [**2**-CO_2CO_2]^{0,c} and [**2**-CO_2CO_2]$^{-1,c}$ being built up during CPE, consistent with the small calculated energy differences between these intermediates (3.5 kcal mol^{-1} between [**2**-CO_2]^0 and [**2**-CO_2CO_2]^{0,c}; 3.0 kcal mol^{-1} between [**2**-CO_2]^0 and [**2**-CO_2CO_2]$^{-1,c}$; Figure 4). Linear [**2**-CO_2CO_2]^0 is not present in detectable amounts, as its diagnostic calculated IR absorption at 1869 cm^{-1} is absent from the experimental CPE monitoring (Figure S5).

Conducting CPE of **2**$^{2+}$ under identical conditions, but with $^{13}CO_2$ gives rise to FT-IR spectra that are qualitatively similar to the ones under $^{12}CO_2$, with the expected shifts due to the isotope labelling. The C=O and C-O stretching vibrations shift by 40-50 and 15-20 cm^{-1} to lower wavenumbers, respectively,[57] when going from $^{12}CO_2$ to $^{13}CO_2$,[37,45] confirming that these IR bands arise from CO_2 (Figure S6). The calculated IR bands of [**2**-$^{13}CO_2{}^{13}CO_2$]$^{-1,c}$ agree well with the experimentally observed ones from CPE (ν (cm^{-1}): experimental (calc.): 1642 (1648), 1564 (1575) and 1279 (1265) cm^{-1}, Figure S7).

The IR-spectroscopic observation of [**2**-CO_2CO_2]$^{-1,c}$ is consistent with a lower rate of C-O bond dissociation compared to that in [**1**-CO_2CO_2]$^{-1,c}$ as evidenced by a higher DFT calculated activation free energy (16.6 kcal mol^{-1} for [**2**-CO_2CO_2]$^{-1,c}$ *vs.* 10.5 kcal mol^{-1} for [**1**-CO_2CO_2]$^{-1,c}$; Figures 3 and 4). The IR signature of [**2**-CO_2CO_2]$^{-1,c}$ is very similar to that of the reported complex Ir$(PMe_3)_3$(Cl)(COOCOO) with a similar metallacycle consisting of two CO_2 molecules in a "head-to-tail" arrangement.[46] The latter was made by the stoichiometric reaction of a low-valent metal precursor and CO_2, and exhibits IR bands at 1725, 1680, 1648 (sh), 1605, and 1290 cm^{-1}.

Further experimental evidence for the presence of cyclic intermediates during the catalytic cycle of **2**$^{2+}$ was sought from ^{13}C NMR analysis after 1h CPE of an CH_3CN solution under an atmosphere of isotopically labeled $^{13}CO_2$ (see ESI). The experiments were repeated multiple times, and while the obtained individual ^{13}C NMR spectra showed qualitative differences, their collective interpretation gave a unified picture of the species involved (Figure S8). First, the DEPT (Distortionless Enhancement by Polarization Transfer) ^{13}C NMR spectra of the samples showed no signals (Figure S9), in the region where Ru-bound carboxylato intermediates derived from $^{13}CO_2$ would be expected. [48,49,59] The absence of such signals in the DEPT ^{13}C NMR spectra ascertain that all resonances observed in ordinary ^{13}C NMR spectra in this region arise from quaternary carbons. In all experiments, the CO_3^{2-}/HCO_3^- byproduct features as a broad resonance at about 160.0 ppm (Figure S8; δ = 160.9 ppm for tetraethylammonium bicarbonate in CD_3CN, Figure S10), while dissolved $^{13}CO_2$ is observed at 125.8 ppm. Consistently observed in all experiments is also a single resonance at ~164.3 ppm, albeit in varying intensity relative to the other signals (Figure S8). It is thus safe to assume that this signal arises from a species that contains only one CO_2-derived ligand, which suggest an assignment to [**2**-CO_2]^0. Other signals that are observed in the ^{13}C NMR spectra emerge in pairs of two, with one such set at ~157.5 ppm and ~165.0 ppm being present in all ^{13}C NMR experiments. Another pair of signals at 167.1 ppm and 169.1 ppm is only observed in some of the experiments. Considering the appearance of these signals in pairs, they are likely to arise from species that contain a C_2O_4–type ligand.

It is important to realize that species observed in the ^{13}C NMR experiments may not be the same as those detected by FT-IR spectroscopy, as, for example, reduced [**2**-CO_2CO_2]$^{-1,c}$ will be oxidized to [**2**-CO_2CO_2]^{0,c} by trace amounts of oxygen during NMR sample preparation. Given this re-oxidation to [**2**-CO_2CO_2]^{0,c}, also [**2**-CO_2CO_2]^0 can be expected in the NMR experiments, as the two species are basically iso-energetic (Figure 4). With this reasoning, the two pairs of signals are tentatively assigned to cyclic [**2**-CO_2CO_2]^{0,c} and linear [**2**-CO_2CO_2]^0.

CONCLUSIONS

In summary, the present work describes an unexplored mechanistic pathway for low-energy C-O bond cleavage in the reductive disproportionation of CO_2 to CO and CO_3^{2-}. Computational work in conjunction with IR and NMR-spectroscopic detection of accumulated reaction intermediates established the involvement of an unprecedented 5-membered metallacyclic intermediate in the catalytic cycle. The formation of the metallacycle is

enabled by the flexible ligation of the polypyridyl ligands, and it is shown that the ligand with the least binding strength to the metal is the one that partially de-coordinates to liberate the coordination site required for metallacycle formation. The Ru center plays a dual role in the catalytic cycle: it acts as a Lewis base and attacks the first CO_2 molecule at an early stage of the cycle, while also acting as an intramolecular Lewis acidic site to stabilize the negative charge of the [**Ru**-CO_2CO_2]^0, thereby leading to the cyclic [**Ru**-CO_2CO_2]^{0,c}. The latter is crucial for energy-conserving turnover, as it allows for a third reduction at a more positive potential than that of the starting complexes $\mathbf{1}^{2+}$ and $\mathbf{2}^{2+}$. The thereby produced [**Ru**-CO_2CO_2]$^{-1,c}$ contains structural features that allow for relatively facile C-O bond cleavage with the calculated activation barrier for this step being dramatically decreased as compared to the 60 kcal mol^{-1} required for C-O bond cleavage in the non-cyclic [**Ru**-CO_2CO_2]^0. Subsequent carbonate liberation and re-ligation of the polypyridine ligand closes the catalytic cycle, and gives the catalyst a good overall stability. The present report is the first of its kind that experimentally observes metallacyclic intermediates during catalytic turnover. Considering its simplicity, it may well be that similar species in other mononuclear catalysts have hitherto been overlooked. At the same time, its identification and operation offer a new design feature that can now be implemented consciously in future catalyst designs.

SUPPORTING INFORMATION

Experimental and computational details, spectra, figures, tables.

AUTHOR INFORMATION

Corresponding Authors

***Mårten Ahlquist** - Department of Theoretical Chemistry and Biology, School of Engineering Sciences in Chemistry, Biotechnology and Health, KTH Royal Institute of Technology, 10691 Stockholm, Sweden; E-mail: ahlqui@kth.se

***Sascha Ott** - Department of Chemistry – Ångström Laboratory, Uppsala University, Box 523, 75120 Uppsala, Sweden; E-mail: Sascha.ott@kemi.uu.se

Authors

Hemlata Agarwala - Department of Chemistry – Ångström Laboratory, Uppsala University, 75120 Uppsala, Sweden

Xiaoyu Chen – Department of Theoretical Chemistry and Biology, School of Engineering Sciences in Chemistry, Biotechnology and Health, KTH Royal Institute of Technology, 10691 Stockholm, Sweden

Julien R. Lyonnet - Department of Chemistry – Ångström Laboratory, Uppsala University, 75120 Uppsala, Sweden

Ben A. Johnson - Department of Chemistry – Ångström Laboratory, Uppsala University, 75120 Uppsala, Sweden

ORCID

Hemlata Agarwala: 0000-0001-7347-3093

Xiaoyu Chen: 0000-0002-7283-8676

Ben A. Johnson: 0000-0002-6570-6392

Mårten Ahlquist: 0000-0002-1553-4027

Sascha Ott: 0000-0002-1691-729X

Present Address

†**Julien R. Lyonnet** – Institute of Chemical Research of Catalonia (ICIQ), The Barcelona Institute of Science and Technology, 43007 Tarragona, Spain; ICREA, 08010 Barcelona, Spain.

Author Contributions

The manuscript was written through contributions of all authors. All authors have given approval to the final version of the manuscript. ‡These authors contributed equally.

Notes

The authors declare no competing financial interest.

ACKNOWLEDGEMENTS

The authors would like to acknowledge the Swedish National Infrastructure for Computing (SNIC), which is funded by the Swedish Research Council (VR) through grant agreement no. 2016-07213, in Linköping (NSC), for the computational resources. The computations were performed under project numbers SNIC2017/1-13, SNIC2018/3-1. SNIC2019/3-6 and SNIC2020/5-41. We acknowledge NordForsk foundation (No. 85378) for the Nordic University hub NordCO_2. MA has been supported by the Swedish Research Council (VR) grant number 2018-05396, and the Knut & Alice Wallenberg (KAW) project CATSS (KAW 2016.0072). XC acknowledges the China Scholarship Council (CSC). HA, and SO acknowledge the Swedish Energy Agency (grant number: 42029-1) for financial support.

REFERENCES

1. Costentin, C.; Drouet, S.; Robert, M.; Savéant, J.-M. Turnover Numbers, Turnover Frequencies, and Overpotential in Molecular Catalysis of Electrochemical Reactions. Cyclic Voltammetry and Preparative-Scale Electrolysis. *J. Am. Chem. Soc.* **2012,** *134* (27), 11235-11242.
2. Azcarate, I.; Costentin, C.; Robert, M.; Savéant, J.-M. Through-Space Charge Interaction Substituent Effects in Molecular Catalysis Leading to the Design of the Most Efficient Catalyst of CO_2-to-CO Electrochemical Conversion. *J. Am. Chem. Soc.* **2016,** *138* (51), 16639-16644.
3. Costentin, C.; Drouet, S.; Robert, M.; Savéant, J.-M. A Local Proton Source Enhances CO_2 Electroreduction to CO by a Molecular Fe Catalyst. *Science* **2012,** *338* (6103), 90-94.
4. Francke, R.; Schille, B.; Roemelt, M. Homogeneously Catalyzed Electroreduction of Carbon Dioxide—Methods, Mechanisms, and Catalysts. *Chem. Rev.* **2018,** *118* (9), 4631-4701.
5. Franco, F.; Pinto, M. F.; Royo, B.; Lloret-Fillol, J. A Highly Active N-Heterocyclic Carbene Manganese(I) Complex for Selective Electrocatalytic CO_2 Reduction to CO. *Angew. Chem. Int. Ed.* **2018,** *57* (17), 4603-4606.
6. Fernández, S.; Franco, F.; Casadevall, C.; Martin-Diaconescu, V.; Luis, J. M.; Lloret-Fillol, J. A Unified Electro- and Photocatalytic CO2 to CO Reduction Mechanism with Aminopyridine Cobalt Complexes. *J. Am. Chem. Soc.* **2020,** *142* (1), 120-133.
7. Merrouch, M.; Benvenuti, M.; Lorenzi, M.; Léger, C.; Fourmond, V.; Dementin, S. Maturation of the [Ni–4Fe–4S] active site of carbon monoxide dehydrogenases. *JBIC Journal of Biological Inorganic Chemistry* **2018,** *23* (4), 613-620.
8. Dobbek, H.; Svetlitchnyi, V.; Gremer, L.; Huber, R.; Meyer, O. Crystal Structure of a Carbon Monoxide Dehydrogenase Reveals a [Ni-4Fe-5S] Cluster. *Science* **2001,** *293* (5533), 1281-1285.
9. Can, M.; Armstrong, F. A.; Ragsdale, S. W. Structure, Function, and Mechanism of the Nickel Metalloenzymes, CO Dehydrogenase, and Acetyl-CoA Synthase. *Chem. Rev.* **2014,** *114* (8), 4149-4174.
10. Elgrishi, N.; Chambers, M. B.; Wang, X.; Fontecave, M. Molecular polypyridine-based metal complexes as catalysts for the reduction of CO_2. *Chem. Soc. Rev.* **2017,** *46* (3), 761-796.
11. Dey, S.; Todorova, T. K.; Fontecave, M.; Mougel, V. Electroreduction of CO_2 to Formate with Low Overpotential using Cobalt Pyridine Thiolate Complexes. *Angew. Chem. Int. Ed.* **2020,** *59* (36), 15726-15733.

12. Ahmed, M. E.; Rana, A.; Saha, R.; Dey, S.; Dey, A. Homogeneous Electrochemical Reduction of CO_2 to CO by a Cobalt Pyridine Thiolate Complex. *Inorg. Chem.* **2020,** *59* (8), 5292-5302.

13. Boutin, E.; Merakeb, L.; Ma, B.; Boudy, B.; Wang, M.; Bonin, J.; Anxolabéhère-Mallart, E.; Robert, M. Molecular catalysis of CO_2 reduction: recent advances and perspectives in electrochemical and light-driven processes with selected Fe, Ni and Co aza macrocyclic and polypyridine complexes. *Chem. Soc. Rev.* **2020,** *49* (16), 5772-5809.

14. Fogeron, T.; Todorova, T. K.; Porcher, J.-P.; Gomez-Mingot, M.; Chamoreau, L.-M.; Mellot-Draznieks, C.; Li, Y.; Fontecave, M. A Bioinspired Nickel(bis-dithiolene) Complex as a Homogeneous Catalyst for Carbon Dioxide Electroreduction. *ACS Catal.* **2018,** *8* (3), 2030-2038.

15. Fogeron, T.; Retailleau, P.; Gomez-Mingot, M.; Li, Y.; Fontecave, M. Nickel Complexes Based on Molybdopterin-like Dithiolenes: Catalysts for CO_2 Electroreduction. *Organometallics* **2019,** *38* (6), 1344-1350.

16. Mouchfiq, A.; Todorova, T. K.; Dey, S.; Fontecave, M.; Mougel, V. A bioinspired molybdenum–copper molecular catalyst for CO_2 electroreduction. *Chem. Sci.* **2020,** *11* (21), 5503-5510.

17. Gonell, S.; Lloret-Fillol, J.; Miller, A. J. M. An Iron Pyridyl-Carbene Electrocatalyst for Low Overpotential CO_2 Reduction to CO. *ACS Catal.* **2021,** *11* (2), 615-626.

18. Gonell, S.; Massey, M. D.; Moseley, I. P.; Schauer, C. K.; Muckerman, J. T.; Miller, A. J. M. The Trans Effect in Electrocatalytic CO_2 Reduction: Mechanistic Studies of Asymmetric Ruthenium Pyridyl-Carbene Catalysts. *J. Am. Chem. Soc.* **2019,** *141* (16), 6658-6671.

19. Gonell, S.; Assaf, E. A.; Duffee, K. D.; Schauer, C. K.; Miller, A. J. M. Kinetics of the Trans Effect in Ruthenium Complexes Provide Insight into the Factors That Control Activity and Stability in CO_2 Electroreduction. *J. Am. Chem. Soc.* **2020,** *142* (19), 8980-8999.

20. Hooe, S. L.; Dressel, J. M.; Dickie, D. A.; Machan, C. W. Highly Efficient Electrocatalytic Reduction of CO_2 to CO by a Molecular Chromium Complex. *ACS Catal.* **2020,** *10* (2), 1146-1151.

21. Franco, F.; Cometto, C.; Nencini, L.; Barolo, C.; Sordello, F.; Minero, C.; Fiedler, J.; Robert, M.; Gobetto, R.; Nervi, C. Local Proton Source in Electrocatalytic CO_2 Reduction with [Mn(bpy–R)$(CO)_3$Br] Complexes. *Chem. Eur. J.* **2017,** *23* (20), 4782-4793.

22. Ngo, K. T.; McKinnon, M.; Mahanti, B.; Narayanan, R.; Grills, D. C.; Ertem, M. Z.; Rochford, J. Turning on the Protonation-First Pathway for Electrocatalytic CO_2 Reduction by Manganese Bipyridyl Tricarbonyl Complexes. *J. Am. Chem. Soc.* **2017,** *139* (7), 2604-2618.

23. Agarwal, J.; Shaw, T. W.; Schaefer, H. F.; Bocarsly, A. B. Design of a Catalytic Active Site for Electrochemical CO_2 Reduction with Mn(I)-Tricarbonyl Species. *Inorg. Chem.* **2015,** *54* (11), 5285-5294.

24. Tignor, S. E.; Shaw, T. W.; Bocarsly, A. B. Elucidating the origins of enhanced CO_2 reduction in manganese electrocatalysts bearing pendant hydrogen-bond donors. *Dalton Trans.* **2019,** *48* (33), 12730-12737.

25. Gotico, P.; Roupnel, L.; Guillot, R.; Sircoglou, M.; Leibl, W.; Halime, Z.; Aukauloo, A. Atropisomeric Hydrogen Bonding Control for CO_2 Binding and Enhancement of Electrocatalytic Reduction at Iron Porphyrins. *Angew. Chem. Int. Ed.* **2020,** *59* (50), 22451-22455.

26. Buss, J. A.; VanderVelde, D. G.; Agapie, T. Lewis Acid Enhancement of Proton Induced CO2 Cleavage: Bond Weakening and Ligand Residence Time Effects. *J. Am. Chem. Soc.* **2018,** *140* (32), 10121-10125.

27. Sen, P.; Mondal, B.; Saha, D.; Rana, A.; Dey, A. Role of 2nd sphere H-bonding residues in tuning the kinetics of CO_2 reduction to CO by iron porphyrin complexes. *Dalton Trans.* **2019,** *48* (18), 5965-5977.

28. Zee, D. Z.; Nippe, M.; King, A. E.; Chang, C. J.; Long, J. R. Tuning Second Coordination Sphere Interactions in Polypyridyl–Iron Complexes to Achieve Selective Electrocatalytic Reduction of Carbon Dioxide to Carbon Monoxide. *Inorg. Chem.* **2020,** *59* (7), 5206-5217.

29. Loipersberger, M.; Zee, D. Z.; Panetier, J. A.; Chang, C. J.; Long, J. R.; Head-Gordon, M. Computational Study of an Iron(II) Polypyridine Electrocatalyst for CO_2 Reduction: Key Roles for Intramolecular Interactions in CO_2 Binding and Proton Transfer. *Inorg. Chem.* **2020,** *59* (12), 8146-8160.

30. Rønne, M. H.; Cho, D.; Madsen, M. R.; Jakobsen, J. B.; Eom, S.; Escoudé, É.; Hammershøj, H. C. D.; Nielsen, D. U.; Pedersen, S. U.; Baik, M.-H.; Skrydstrup, T.; Daasbjerg, K. Ligand-Controlled Product Selectivity in Electrochemical Carbon Dioxide Reduction Using Manganese Bipyridine Catalysts. *J. Am. Chem. Soc.* **2020,** *142* (9), 4265-4275.

31. Margarit, C. G.; Schnedermann, C.; Asimow, N. G.; Nocera, D. G. Carbon Dioxide Reduction by Iron Hangman Porphyrins. *Organometallics* **2019,** *38* (6), 1219-1223.

32. Madsen, M. R.; Jakobsen, J. B.; Rønne, M. H.; Liang, H.; Hammershøj, H. C. D.; Nørby, P.; Pedersen, S. U.; Skrydstrup, T.; Daasbjerg, K. Evaluation of the Electrocatalytic Reduction of Carbon Dioxide using Rhenium and Ruthenium Bipyridine Catalysts Bearing Pendant Amines in the Secondary Coordination Sphere. *Organometallics* **2020,** *39* (9), 1480-1490.

33. Amanullah, S.; Saha, P.; Nayek, A.; Ahmed, M. E.; Dey, A. Biochemical and artificial pathways for the reduction of carbon dioxide, nitrite and the competing proton reduction: effect of 2nd sphere interactions in catalysis. *Chem. Soc. Rev.* **2021**.

34. Hammouche, M.; Lexa, D.; Momenteau, M.; Saveant, J. M. Chemical catalysis of electrochemical reactions. Homogeneous catalysis of the electrochemical reduction of carbon dioxide by iron("0") porphyrins. Role of the addition of magnesium cations. *J. Am. Chem. Soc.* **1991,** *113* (22), 8455-8466.

35. Bhugun, I.; Lexa, D.; Savéant, J.-M. Catalysis of the Electrochemical Reduction of Carbon Dioxide by Iron(0) Porphyrins. Synergistic Effect of Lewis Acid Cations. *The Journal of Physical Chemistry* **1996,** *100* (51), 19981-19985.

36. Isegawa, M.; Sharma, A. K. CO_2 reduction by a Mn electrocatalyst in the presence of a Lewis acid: a DFT study on the reaction mechanism. *Sust. Energy & Fuels* **2019,** *3* (7), 1730-1738.

37. Sampson, M. D.; Kubiak, C. P. Manganese Electrocatalysts with Bulky Bipyridine Ligands: Utilizing Lewis Acids To Promote Carbon Dioxide Reduction at Low Overpotentials. *J. Am. Chem. Soc.* **2016,** *138* (4), 1386-1393.

38. Johnson, B. A.; Maji, S.; Agarwala, H.; White, T. A.; Mijangos, E.; Ott, S. Activating a Low Overpotential CO_2 Reduction Mechanism by a Strategic Ligand Modification on a Ruthenium Polypyridyl Catalyst. *Angew. Chem. Int. Ed.* **2016,** *55* (5), 1825-1829.

39. Johnson, B. A.; Agarwala, H.; White, T. A.; Mijangos, E.; Maji, S.; Ott, S. Judicious Ligand Design in Ruthenium Polypyridyl CO_2 Reduction Catalysts to Enhance Reactivity by Steric and Electronic Effects. *Chem. Eur. J.* **2016,** *22* (42), 14870-14880.

40. Ben Hadda, T.; Le Bozec, H. Synthesis and characterization of ruthenium(II) complexes containing the new tridentate ligand 4,4′,4″-tri-tert-butyl-terpyridine. *Inorg. Chim. Acta* **1993,** *204* (1), 103-107.

41. Gennaro, A.; Isse, A. A.; Vianello, E. Solubility and electrochemical determination of CO_2 in some dipolar aprotic solvents. *J. Electroanal. Chem. Interfacial Electrochem.* **1990,** *289* (1), 203-215.

42. Chen, Z.; Chen, C.; Weinberg, D. R.; Kang, P.; Concepcion, J. J.; Harrison, D. P.; Brookhart, M. S.; Meyer, T. J. Electrocatalytic reduction of CO_2 to CO by polypyridyl ruthenium complexes. *Chem. Commun.* **2011,** *47* (47), 12607-12609.

43. Sullivan, B. P.; Bolinger, C. M.; Conrad, D.; Vining, W. J.; Meyer, T. J. One- and two-electron pathways in the electrocatalytic reduction of CO_2 by fac-Re(bpy)$(CO)_3$Cl (bpy = 2,2′-bipyridine). *J. Chem. Soc., Chem. Commun.* **1985,** (20), 1414-1416.

44. Agarwal, J.; Fujita, E.; Schaefer, H. F.; Muckerman, J. T. Mechanisms for CO Production from CO_2 Using Reduced Rhenium Tricarbonyl Catalysts. *J. Am. Chem. Soc.* **2012,** *134* (11), 5180-5186.

45. Machan, C. W.; Chabolla, S. A.; Yin, J.; Gilson, M. K.; Tezcan, F. A.; Kubiak, C. P. Supramolecular Assembly Promotes the

Electrocatalytic Reduction of Carbon Dioxide by Re(I) Bipyridine Catalysts at a Lower Overpotential. *J. Am. Chem. Soc.* **2014,** *136* (41), 14598-14607.

46. Herskovitz, T.; Guggenberger, L. J. Carbon dioxide coordination chemistry. The structure and some chemistry of the novel carbon dioxide addition product chlorobis(carbon dioxide)tris(trimethylphosphine)iridium. *J. Am. Chem. Soc.* **1976,** *98* (6), 1615-1616.

47. Jurd, P. M.; Li, H. L.; Bhadbhade, M.; Field, L. D. Fe(0)-Mediated Reductive Disproportionation of CO_2. *Organometallics* **2020,** *39* (10), 2011-2018.

48. Feller, M.; Gellrich, U.; Anaby, A.; Diskin-Posner, Y.; Milstein, D. Reductive Cleavage of CO_2 by Metal–Ligand-Cooperation Mediated by an Iridium Pincer Complex. *J. Am. Chem. Soc.* **2016,** *138* (20), 6445-6454.

49. Langer, J.; Imhof, W.; Fabra, M. J.; García-Orduña, P.; Görls, H.; Lahoz, F. J.; Oro, L. A.; Westerhausen, M. Reversible CO_2 Fixation by Iridium(I) Complexes Containing Me_2PhP as Ligand. *Organometallics* **2010,** *29* (7), 1642-1651.

50. Kempe, R.; Sieler, J.; Walther, D.; Reinhold, J.; Rommel, K. Aktivierung von CO_2 an Übergangsmetallzentren: Zum Ablauf der CO_2-Reduktion an Nickel(0)-Fragmenten. *Z. Anorg. Allg. Chem.* **1993,** *619* (6), 1105-1110.

51. Dahlenburg, L.; Prengel, C. Metallorganische verbindungen des iridiums und rhodiums: XXIX. CO_2-transformationen am trisphosphanrhodium(I)-komplex $Rh(4\text{-}MeC_6H_4)[t\text{-}BuP(CH_2CH_2CH_2PPh_2)_2]$. *J. Organomet. Chem.* **1986,** *308* (1), 63-71.

52. Carmona, E.; Gonzalez, F.; Poveda, M. L.; Marin, J. M.; Atwood, J. L.; Rogers, R. D. Reaction of cis-$[Mo(N_2)_2(PMe_3)_4]$ with carbon dioxide. Synthesis and characterization of products of disproportionation and the x-ray structure of a tetrametallic mixed-valence Mo(II)-Mo(V) carbonate with a novel mode of carbonate binding. *J. Am. Chem. Soc.* **1983,** *105* (10), 3365-3366.

53. Lucarini, F.; Fize, J.; Morozan, A.; Marazzi, M.; Natali, M.; Pastore, M.; Artero, V.; Ruggi, A. Insights into the mechanism of photosynthetic H_2 evolution catalyzed by a heptacoordinate cobalt complex. *Sust. Energy & Fuels* **2020,** *4* (2), 589-599.

54. Leung, J. J.; Warnan, J.; Ly, K. H.; Heidary, N.; Nam, D. H.; Kuehnel, M. F.; Reisner, E. Solar-driven reduction of aqueous CO_2 with a cobalt bis(terpyridine)-based photocathode. *Nature Catal.* **2019,** *2* (4), 354-365.

55. Aroua, S.; Todorova, T. K.; Mougel, V.; Hommes, P.; Reissig, H.-U.; Fontecave, M. New Cobalt-Bisterpyridyl Catalysts for Hydrogen Evolution Reaction. *ChemCatChem* **2017,** *9* (12), 2099-2105.

56. Cheng, S. C.; Blaine, C. A.; Hill, M. G.; Mann, K. R. Electrochemical and IR Spectroelectrochemical Studies of the Electrocatalytic Reduction of Carbon Dioxide by $[Ir_2(dimen)_4]^{2+}$ (dimen = 1,8-Diisocyanomenthane). *Inorg. Chem.* **1996,** *35* (26), 7704-7708.

57. Jegat, C.; Fouassier, M.; Tranquille, M.; Mascetti, J.; Tommasi, I.; Aresta, M.; Ingold, F.; Dedieu, A. Carbon dioxide coordination chemistry. 3. Vibrational, NMR, theoretical studies of (carbon dioxide)bis(tricyclohexylphosphine)nickel. *Inorg. Chem.* **1993,** *32* (7), 1279-1289.

58. The remaining calculated peaks at 1695 cm^{-1} and 1291 cm^{-1} for $[\mathbf{2}\text{-}CO_2CO_2]^{-1,c}$ are masked by the CO_3^{2-}/HCO_3^{2-} IR bands centered at 1686 cm^{-1} and 1301 cm^{-1} (Figures S4d and 3b).

59. Arikawa, Y.; Nakamura, T.; Ogushi, S.; Eguchi, K.; Umakoshi, K. Fixation of atmospheric carbon dioxide by ruthenium complexes bearing an NHC-based pincer ligand: formation of a methylcarbonato complex and its methylation. *Dalton Trans.* **2015,** *44* (12), 5303-5305.

Table of Contents